AIMS Energy, 13(3): 517–539.
DOI: 10.3934/energy.2025020
Received: 03 March 2025
Revised: 09 May 2025
Accepted: 20 May 2025
Published: 28 May 2025

https://www.aimspress.com/journal/energy

Research article

A wind power prediction model with meteorological time delay and power characteristic

Feng Tian*

Shenyang Institute of Engineering, Shenyang 110136, China

* **Correspondence:** Email: Tfeng_mailbox@163.com.

Abstract: Wind energy, as a widely distributed, pollution-free energy, is strongly supported by the government. Accurate wind power forecasting technology ensures the balance of the power system and enhances the security of the system. In this paper, a wind power prediction model with the improved long short-term memory (LSTM) network and Adaboost algorithm was constructed based on the mismatch of data and power climb. This method was based on mutual information (MI) and power division (PD), named MI-PD-AdaBoost-LSTM. MI was used for quantifying the time delay between variables and power. Furthermore, to solve the relationship between wind speed and power in different weather fluctuation processes, the method of power fluctuation process division was proposed. Moreover, the asymmetric loss function of AdaBoost-LSTM was constructed to deal with the asymmetric characteristics of wind power. An improved artificial bee colony (ABC) algorithm, which overcame the local optimal problem, was used to optimize the asymmetric loss function parameters. Finally, the performance of different deep learning prediction models and the proposed prediction model was analyzed in the experiment. Numerical simulations showed that the proposed algorithm effectively improves the power prediction accuracy with different time scales and seasons. The designed model provides guidance for wind farm power prediction.

Keywords: wind power prediction; renewable energy; deep learning; wind power asymmetry characteristics; optimization algorithm

1. Introduction

Wind power generation has become the most extensive renewable energy in the world because of its low construction cost and pollution-free advantages. However, wind power is limited due to inherent characteristics such as randomness, volatility, and intermittency. The accurate prediction of wind power can provide a reference for grid dispatching.

As the world continues to face the century's problem of climate change and resource depletion, the development of renewable energy is receiving increasing attention. In particular, renewable energy is an alternative to fossil energy with zero emissions and high economic efficiency. Photovoltaics and wind power provide an economical and environmentally friendly solution to these problems while meeting the growing demand for electricity. Wind power costs far less than traditional fossil fuels. Wind power technology is highly developed and has become a key focus in the energy industry. Compared with traditional energy sources, wind energy is widely recognized by countries for its clean and environmental protection characteristics. In the last decade, the proportion of thermal power in China has dropped from 75% to 60%, while the proportion of wind power will gradually increase. Additionally, the land and offshore wind energy potential in China is around 1.2 billion kilowatts, indicating abundant wind resources [1].

Wind power is mainly affected by different weather conditions, especially wind speed and direction. It will have a certain impact on the system, such as voltage and frequency stability. Therefore, accurate wind power prediction can estimate the future power output and ensure the stable operation of the power system. In recent years, the curtailment rate of wind power has decreased significantly. However, compared with countries with mature wind power technology, there is room for improvement. This indicates that China needs to further strengthen wind power forecasting research to improve the utilization efficiency of wind power and reduce the wind curtailment phenomenon [2]. Accurate power prediction can improve the reliability and economy of wind power. Wind power prediction results can be used to schedule maintenance to maximize the efficiency of wind farm operations.

The technology of wind power prediction is a significant research topic. Data-driven methods, including deep learning and statistics, have been proven to be effective by many scholars [3–5]. However, due to the randomness of wind power generation and the matching between power generation and meteorological data, wind power generation faces many challenges.

With the enrichment of artificial intelligence theory, traditional intelligent algorithms such as machine learning and optimization theory have shortcomings in wind power prediction. Therefore, scholars have proposed a method to improve the accuracy by combining the improved optimization algorithm [6–8]. Among those, the ant colony algorithm and neural network also have some disadvantages when optimizing the wind power prediction model, such as local optimal solutions and overfitting. Researchers have been looking for better solutions to these problems. Therefore, advanced prediction models have been developed.

Gu et al. proposed the random Forest (RF) model to predict the wind power generation model [9]. Liao et al. combined fuzzy decomposition with LSTM and compared the performance with other forecasting models which demonstrates the superiority of their method [10]. Lin et al. proposed an adaptively driven ultra-short-term wind power prediction model. Intelligent algorithms are applied to optimize the extreme learning machine to improve the prediction accuracy and efficiency [11]. He et al. developed a hybrid prediction framework based on classification models and wind power ramp events. Simulation results showed that this prediction method outperformed traditional

methods [12]. Wang et al. proposed a short-term wind power prediction hybrid model. The experimental results show that the accuracy and stability of wind power prediction have been effectively improved in multiple scenarios and time scales [13]. Sun et al. proposed a data-driven online prediction method for wind power generation based on wind power generation wake, which was trained using acoustic data [14]. Safari et al. addressed the issue of chaotic front-end decomposition algorithms by proposing a method that uses singular spectrum analysis and chaos time series analysis for optimization, which showed favorable results [15]. An improved prediction model for LSTM was proposed and constructed by Zhou et al., and their experiments showed the superiority of this method [16]. Considering the uncertainties and anomalies of the original data, Wang et al. focused on processing the data, and then optimized the hyperparameters of the deep learning model to improve the accuracy of the prediction [17]. A novel discrete grey Bernoulli model designed for renewable energy prediction was proposed. It addresses challenges like nonlinearity, poor information, and time lag in renewable energy data [18].

Based on the above analysis, meteorological data provided by nearby public weather stations or wind farms with numerical weather prediction (NWP) are used to build data-driven models. First, according to the historical power curve of the target station and the data in NWP, the meteorological data is processed to solve the problem of meteorological data deviation of the model. Second, the power is divided into different fluctuation processes. Third, LSTM is adopted as the base learner to predict the power. Additionally, the AdaBoost algorithm is used to solve the defects of the model with different data. Finally, the results show that the prediction model performs well. The model performs well in all evaluation indices and can accurately capture the trend and rule of the wind power curve.

2. Time correlation of meteorological information and the division of power process

2.1. Time correlation of meteorological information-power

Within a certain range, wind power exhibits spatial correlation with meteorological factors. In wind farms, there is a time delay between the power output of different turbines and meteorological conditions. Therefore, the weather data is corrected for the time delay characteristic caused by the geographical position, which improves the prediction accuracy. In this paper, the historical meteorological information is shifted to maximize its correlation with the power output curve, thus determining the corresponding time shift. MI is used to characterize the correlation between the main meteorological information and power. The delay with the highest correlation coefficient is selected to calculate the optimal time delay.

As an application of information theory in the direction of machine learning, MI has attracted attention for its excellent variable distribution independence and data space invariance. It reflects the dependence of two variables based on information entropy [19]. As the core of traditional time delay calculation methods, MI can represent the linear correlation of two variables. There are time series a and b, whose sequence length is n. If there is a time delay between sequences, the cross-correlation function can be expressed as:

$$\phi_{ab}(k)=\frac{1}{n-k}\cdot\frac{\sum_{i=1}^{n-k}(a_i-\bar{a})(b_{i+k}-\bar{b})}{\sqrt{\sum_{i=1}^{n}(a_i-\bar{a})^2}\sqrt{\sum_{i=1}^{n}(b_i-\bar{b})^2}},k=0,1,\cdots,n-1 \tag{1}$$

where $\bar{a}$ and $\bar{b}$ are the mean values of the selected sequence, and $\phi_{ab}(k)$ is the similarity coefficient of evaluation. Thus, the time delay is calculated as

$$\tau=argmax\{\phi_{ab}(k),k=0,1,\ldots,n\} \tag{2}$$

Similarly, if *k* is negative, then *b* lags behind *a*. The cross-correlation function of the sequence is

$$\phi_{ab}(k)=\frac{1}{n+k}\cdot\frac{\sum_{i=1-k}^{n}(a_i-\bar{a})(b_{i+k}-\bar{b})}{\sqrt{\sum_{i=1}^{n}(a_i-\bar{a})^2}\sqrt{\sum_{i=1}^{n}(b_i-\bar{b})^2}},k=-n+1,-n+2,\cdots,0 \tag{3}$$

The overall delay is estimated as:

$$\tau=argmax\{|\phi_{ab}(k)|,k=-n+1,-n+2,\cdots,0\} \tag{4}$$

The optimal time delay of meteorological information and power can be determined by Eqs (1–4). The principle of the time delay model is shown in Figure 1.

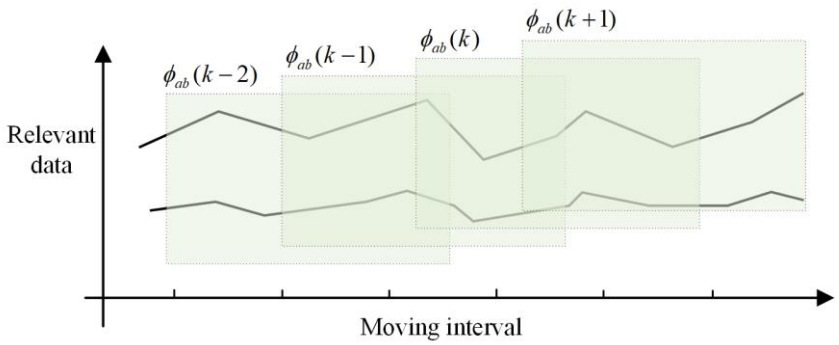

Figure 1. The model of time delay.

2.2. Classification of wind power characteristics

Wind power curves are generated by wind farm data. Further, the power curve is divided into three fluctuation processes, which are the small range power fluctuation process, P_s, the moderate range power fluctuation process, P_m, and the large range power fluctuation process, P_l. Based on the

curve, the PD threshold is determined to ensure the relationship between characteristics and other factors. The value starts from the minimum value of a power threshold and reaches the maximum value above the power threshold. It is worth noting that there may be multiple peaks in the partitioning process, as shown in Figure 2. Mathematical expressions are defined as:

$$P_{wind} = \begin{cases} P_s, & P \le \xi_s \\ P_m, & \xi_s \le P \le \xi_l \\ P_l, & \xi_l \le P \end{cases} \tag{5}$$

where ξ_s is the defined small range value. ξ_l is a large range of values. P is the maximum value in the power range. In this paper, the power fluctuation range ξ is determined through the power gradient.

$$\xi = \frac{\sum_{t}^{T} \Delta P(t)}{P_{\text{rated}}} \tag{6}$$

where ΔP represents the difference in power fluctuation within a unit of time. P_{rated} is the rated power.

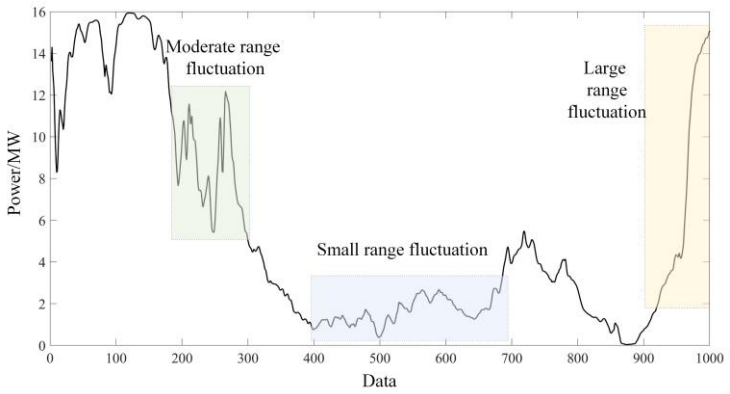

Figure 2. Power fluctuation process.

3. The model of AdaBoost-LSTM

3.1. The principles of LSTM

Compared to traditional RNNs, LSTM introduces memory cells and gate mechanisms, which effectively capture and process time series data [10]. As a result, LSTM is chosen for wind power prediction in this paper. The LSTM is structured as follows:

$$f_t = \sigma\left(W_f x_t + U_f h_{t-1} + b_f\right) \tag{7}$$

$$i_t = \sigma\left(W_i x_t + U_i h_{t-1} + b_i\right) \tag{8}$$

$$\bar{c} = \tanh\left(W_c x_t + U_c h_{t-1} + b_c\right) \tag{9}$$

$$c_t = f_t \otimes c_{t-1} + i_t \otimes \bar{c}_t \tag{10}$$

$$h_t = \sigma\left(W_o x_t + U_o h_{t-1} + b_o\right) \otimes \tanh\left(c_t\right) \tag{11}$$

where f_t, $\bar{c}$, and x_t are forgetting gates, input gates, and neural network inputs, respectively. h_{t-1} is the output of the previous neural network. σ is a sigmoid function. W and b are weighted and biased in different network layers, respectively. tanh is an activation function. $\otimes$ is number multiplication.

If there are anomalies in the wind power, the prediction error will be large, which will reduce the overall performance of the model. Therefore, we discuss the influence of outliers on the prediction model and design a new optimization criterion to improve the prediction accuracy. The existing wind power prediction methods often assume that the error distribution follows a Gaussian distribution and use MSE as the loss function. However, due to the influence of random factors such as weather and temperature, the error distribution of real wind power data does not meet the Gaussian distribution. Therefore, the asymmetric loss function is constructed as a loss function in this paper.

The asymmetric loss function is designed as follows:

$$L_{\alpha,\beta}\left(y,\hat{y}\right) = \begin{cases} \alpha\left|y-\hat{y}\right|^{\beta} & y \geq \hat{y} \\ \left(1-\alpha\right)\left|y-\hat{y}\right|^{\beta} & y < \hat{y} \end{cases} \tag{12}$$

where α and β are the related parameters of the asymmetric loss function, which control the performance of the LSTM according to the data characteristics. y and $\hat{y}$ are the actual and predicted values, respectively.

3.2. Improved ABC

In practical applications, it is a difficult problem to select the optimal parameters of the asymmetric loss function. Next, an efficient improved ABC optimization algorithm is designed to solve this problem by searching for the optimal parameters. The ABC algorithm is accomplished through the close cooperation of three kinds of bees: Hired bees, follower bees, and scout bees.

In the ABC algorithm, there are four major parts:

(1) Initialize the population. The maximum number of iterations (LIM), the maximum number of abandoned nectar sources (Limit), and the number of initial populations N are set. The initial solution is generated.

(2) Population renewal. The quality of the original nectar source was compared by randomly selecting adjacent nectar sources and old nectar sources. The high-quality nectar source is selected.

(3) Probability selection. The information about hired bees is probabilized to determine whether to update the honey source and conduct a search.

(4) Population elimination. If a solution does not improve within the maximum number of iterations, the hired bees will become scout bees and randomly search for new honey sources again.

The traditional ABC algorithm has the advantages of simple operation and fewer control parameters. However, when applied to actual project engineering, this algorithm is more prone to local optimal values, and the convergence speed is normal. This indicates that the traditional artificial bee colony algorithm has a strong search ability, but its development ability needs to be improved.

In this paper, three parts of population renewal, probability selection, and elimination strategy are improved to enhance the performance of the ABC algorithm. On the basis of retaining strong searching ability, the improved algorithm strengthens development ability and finds the optimal solution to the problem more efficiently

3.2.1. Population updating based on information feedback

As an important part of the bee colony algorithm, population updating includes two parts: Selection and renewal, which have a great influence on the whole optimization process. A random approach is employed in the traditional artificial bee colony algorithm for population renewal. Random individuals and random components enhance the robustness of the ABC algorithm. Random individuals influence fair competition. The random component has a great influence on the accuracy of the solution. The random selection of the individual components increases the local optimal solution and increases the operational complexity. To solve the problem better, the mechanism of the individual component recorder (CH) was introduced in order to fully search the individual component to improve the quality of the honey source. CH = 1 indicates improvement and CH = 0 indicates no improvement. If it is not raised, the component can continue to be randomly selected. In this way, the accuracy can be effectively improved.

The updated formula after improvement is as follows:

$$x_{pq} = x_{pq} + \phi^{*}(x_{q}^{best} - x_{kq}) \tag{13}$$

where $\phi^{*} \in [-1,1]$. x_{pq} is the *qth* component of the newly generated solution. x_{q}^{best} is the *qth* component of the optimal solution. x_{kq} is the component of the solution to be updated.

3.2.2. Improvement of fitness function

In the traditional probability selection formula, if the fitness value is very small, infinitely close to 0, but there are some differences, the traditional formula is not distinguishable enough, and the fitness value will be infinitely close to 1, which will lead to the same final selection probability value.

To solve the above problems, a logarithmic effect is introduced to amplify the difference of fitness values. By distinguishing differences, probabilities are generated, and better-performing individuals are updated. When the accuracy of the optimal individual reaches a certain range, the original algorithm can't distinguish the difference. Then, the improved formula based on a logarithmic effect is used to evaluate. The improved fitness function formula is as follows:

$$F_i = \frac{0.1}{0.1 + \frac{1}{|\log_{10} fit_i|}}, 0 \leqslant fit_i \leqslant 10^{-\alpha} \tag{14}$$

where α is to set the recognition accuracy of the solution, and the range is 4–8. fit_1, fit_2 and fit_3 are converted into probabilistic information by the above formula. As shown in Eq (14)

$$\begin{aligned} fit_1 &= 1\times10^{-20} \xrightarrow{f_7} F_1 \approx 0.67 \xrightarrow{f_3} P_1 \approx 0.27 \\ fit_2 &= 1\times10^{-50} \xrightarrow{f_7} F_2 \approx 0.83 \xrightarrow{f_3} P_2 \approx 0.35 \\ fit_3 &= 1\times10^{-100} \xrightarrow{f_7} F_3 \approx 0.91 \xrightarrow{f_3} P_3 \approx 0.38 \end{aligned} \tag{15}$$

3.2.3. Optimally guided elimination update mechanism

When a honey source does not improve after a set number of iterations, it will enter the population elimination process. The basic phase-out mechanism has been improved in this section. In the process of randomly generating new individuals after discarding individuals, the new individuals are generated by crossing between eliminated individuals and optimal individuals. This method can effectively solve the above problems and significantly enhance the optimization effect of the experiment. The crossover formula is:

$$x_{nm} = x_m^{best} + \phi^* \left(x_m^{best} + x_{lm} \right) \tag{16}$$

where x_{pq} is the newly generated individual of the qth component, x_q^{best} is the newly generated individual of the qth component, and x_{kq} is the individual component to be eliminated.

The improved ABC process with information feedback mechanism, logarithmic effect, and introduction of optimally guided elimination update function is shown in Figure 3. The improved ABC algorithm retains the advantages of the algorithm and reduces the risk of falling into the local optimal solution.

The processes of improved ABC are summarized in Algorithm 1 below:

Algorithm 1: Improved ABC

Input: LIM, N, Limit, CH, number of parameters, lower bound, upper bound
Output: optimal parameter

Initialize: α and β, CH

For iteration = 1 to LIM **do**
Population updating: update by Eq (13)
Fitness function: calculation by Eqs (14) and (15)
Guided elimination update mechanism：Individual elimination and renewal by Eq (16)
end
Return optimal parameter

3.3. AdaBoost Algorithm

AdaBoost, characterized by flexibility, can be used with a variety of weak classifiers. The main advantage of the algorithm is its simple structure. The final strong classifier is the weighted sum of all the weak classifiers, where the weight of each classifier is determined by its performance in training [20]. AdaBoost can significantly improve classification accuracy and has a high tolerance for noise and overfitting.

The r data sets are divided based on power fluctuations. Data set p is $\left(x_{p1}, y_{p1}\right), \left(x_{p2}, y_{p2}\right), \cdots, \left(x_{pm}, y_{pm}\right), \cdots, \left(x_{pN}, y_{pN}\right)$. The LSTM is used as a weak learner and the steps for AdaBoost are as follows:

(1) Initialize the weight of the p th data set. The weights are equally distributed:

$$W_m^p = \frac{1}{N}, m = 1, 2, 3, \ldots, N \tag{17}$$

(2) The overall error of calculating the error weight:

$$f_{p,j} = \sum_{m=1}^{N} W_{m,j}^p I\left[y_{m,p} \neq O_{p,j}\left(x_{m,p}\right)\right] \tag{18}$$

where $W_{m,j}^p$ is the weight of the j th iteration of the m sample in the dataset. Furthermore, $O_{p,j}\left(x_{m,p}\right)$ is the output of the LSTM.

$$e_{p,j} = \frac{f_{p,j}}{\sum_{m=1}^{N} W_{m,j}^p} \tag{19}$$

$$\alpha_{p,j} = \log\left(\frac{1-e_{p,j}}{e_{p,j}}\right) \tag{20}$$

$$W_{m,j+1} = W_{m,j} \exp\left[\alpha_{p,j} * I\left(y_{m,p} \neq O_{p,j}\left(x_{m,p}\right)\right)\right] \tag{21}$$

(3) Finally, the different model output results are recombined with weights as the final output.

$$O_p\left(x_{m,p}\right) = \operatorname{argmax}\left[\sum_{j=1}^{J} \alpha_{p,j} O_{p,j}\left(x_{m,p}\right)\right] \tag{22}$$

In summary, the power forecasting model presented in this paper is shown in Figure 3. The different data is selected for training. The time delay of factors is calculated based on MI. Additionally, the wind power fluctuation process is divided into three processes: Small range fluctuation, medium range fluctuation, and large range fluctuation. Different data type subsets of power are allocated

according to the different fluctuation processes. Three AdaBoost-LSTM sub-prediction models are constructed according to data. Finally, the prediction models are arranged according to the time series.

The power prediction model constructed is as follows:

(1): Different meteorological data of the wind farm are input.

(2): The time delay correlation between inputs and outputs is analysed by the MI.

(3): Considering the power characteristics of the fan, different power curves and related input data are divided.

(4): Construct AdaBoost-LSTM model with different power features.

(5): The improved ABC algorithm is used to optimize the parameters α and β, where $\alpha_{\min}$ and $\alpha_{\max}$ are the intervals initialized by α. $\beta_{\min}$ and $\beta_{\max}$ are the intervals initialized by β.

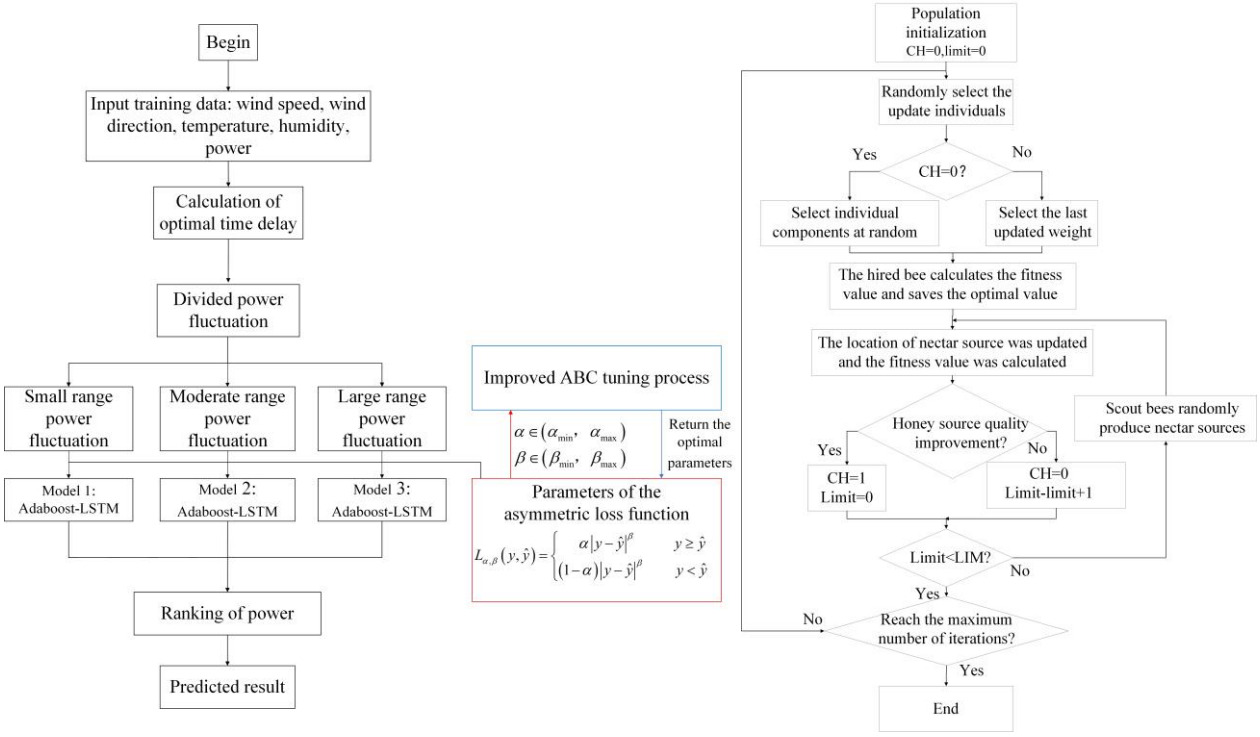

(a) hybrid model (b) The flowchart of the improved ABC

Figure 3. The architecture of the hybrid model.

3.4. Evaluation indicators

A comprehensive scientific evaluation of different prediction models is carried out using standard evaluation indices. Specifically, the three evaluation indicators (MAE, MAPE, and RMSE) are as follows:

$$y_{MAE} = \frac{1}{N}\sum_{t=1}^{N}\left|\hat{y}_t - y_t\right| \tag{23}$$

$$y_{MAPE} = \frac{1}{N}\sum_{t=1}^{N}\left|\frac{\hat{y}_t - y_t}{y_t}\right| \tag{24}$$

$$y_{RMSE} = \sqrt{\frac{1}{N}\sum_{t=1}^{N}(\hat{y}_t - y_t)} \tag{25}$$

where $\hat{y}_t$ is the output of the model. y_t is the actual power.

4. Experimental analysis

The actual data of an inland wind farm and a coastal wind farm in Liaoning province are used in this experiment. The data is from Jan. 1, 2021 to Dec. 31, 2021. The improved ABC algorithm is set as follows: $LIM = 500$, $Limit = 100$ and $N = 70$.

4.1. Determination based on the time delay of the inland wind farm

Wind power delay coefficient is determined by MI, and the calculated results are shown in Figure 4. The correlation coefficients are different for the time delay of multiple time scales. The correlation coefficients with different time delays differ. MI can effectively extract the dynamic change of delay at different time points. Therefore, the prediction model has higher accuracy and stability. The optimal time delay for different variables can be obtained from Table 1. After calculation, the time delay of wind speed and direction is 5 min. The time delay of air pressure is 0 min, and the time delay of humidity is 10 min. Different from the above, the time lead of temperature is 5 min.

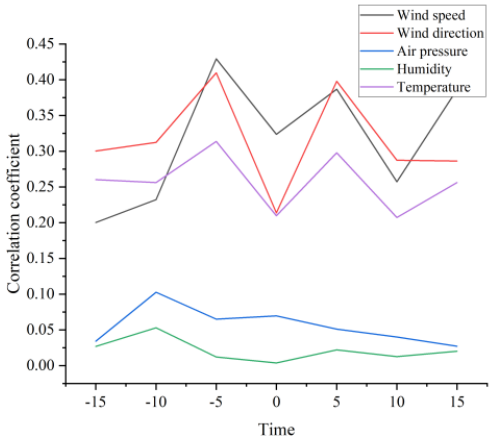

Figure 4. The time delay of the input.

Table 1. Correlation coefficients of different time delays in the inland region.

Variables	Time shift						
	−15 min	−10 min	−5 min	0	5 min	10 min	15 min
Wind speed	0.2001	0.2323	0.4293	0.3236	0.3867	0.2573	0.3861
Wind direction	0.3001	0.3123	0.4095	0.2136	0.3977	0.2873	0.2861
Air pressure	0.034	0.1026	0.065	0.0695	0.0509	0.0401	0.0271
Humidity	0.0268	0.0529	0.012	0.0037	0.0219	0.0126	0.0202
Temperature	0.2601	0.2562	0.3136	0.2095	0.2977	0.2073	0.2561

4.2. Sensitivity analysis of the inland wind farm

The influence of parameters α and β on the prediction performance of the asymmetric loss function is analyzed. α=1 and α=2. β is selected as 0.3–0.7 with an interval of 0.1. The performance indicators in different seasons and different time scales are shown in Table 2. There are differences in the performance of the models with different datasets in the above analysis. For example, in spring, the parameter is selected as $\alpha=1$, $\beta=0.5$. In summer, $\alpha=1$ and $\beta=0.5$ are chosen. In autumn, $\alpha=1$, $\beta=0.7$ is chosen. In winter, $\alpha=1$, $\beta=1$ is chosen. Since the parameters can be set to different values. Therefore, the improved ABC is designed to optimize parameters α and β, where $\alpha_{\min}$=1, $\alpha_{\max}$=2, $\beta_{\min}$=0 and $\beta_{\max}$=1. The optimization results of inland region with multiple time steps and different seasons are shown in Tables 3 and 4. The convergence performance of the improved ABC and the traditional ABC is shown in Figure 5. It can be seen that the improved ABC optimization algorithm has a faster convergence speed.

Table 2. Performance comparison of loss function parameters for different seasons in the inland region.

Season	β	$\alpha=1$			$\alpha=2$		
		MAE	MAPE	RMSE	MAE	MAPE	RMSE
Spring	0.3	0.1029	0.1375	0.1243	0.1059	0.1285	0.1271
	0.4	0.1106	0.1327	0.1179	0.1053	0.1348	0.1223
	0.5	0.1035	0.1374	0.1248	0.1120	0.1339	0.1175
	0.6	0.1058	0.1298	0.1215	0.1093	0.1282	0.1178
	0.7	0.1083	0.1315	0.1254	0.1062	0.1287	0.1187
Summer	0.3	0.1021	0.0096	0.1201	0.1046	0.0150	0.1222
	0.4	0.1044	0.0128	0.1203	0.1005	0.0170	0.1245
	0.5	0.1003	0.0081	0.1214	0.1074	0.0127	0.1182
	0.6	0.1088	0.0162	0.1183	0.1004	0.0100	0.1221
	0.7	0.1061	0.0120	0.1154	0.1095	0.0102	0.1157
Autumn	0.3	0.1048	0.0143	0.1217	0.1037	0.0101	0.1229
	0.4	0.1031	0.0162	0.1165	0.1015	0.0131	0.1188
	0.5	0.1061	0.0111	0.1174	0.1087	0.0173	0.1159
	0.6	0.1014	0.0143	0.1222	0.1006	0.0162	0.1192
	0.7	0.0997	0.0163	0.1204	0.1074	0.0115	0.1226
Winter	0.3	0.1096	0.0909	0.1159	0.1079	0.0864	0.1228
	0.4	0.1054	0.0847	0.1241	0.1026	0.0931	0.1244
	0.5	0.1050	0.087	0.1186	0.1028	0.0924	0.1169
	0.6	0.1037	0.0874	0.1182	0.1104	0.0853	0.1161
	0.7	0.1012	0.0923	0.1206	0.1065	0.0834	0.1217

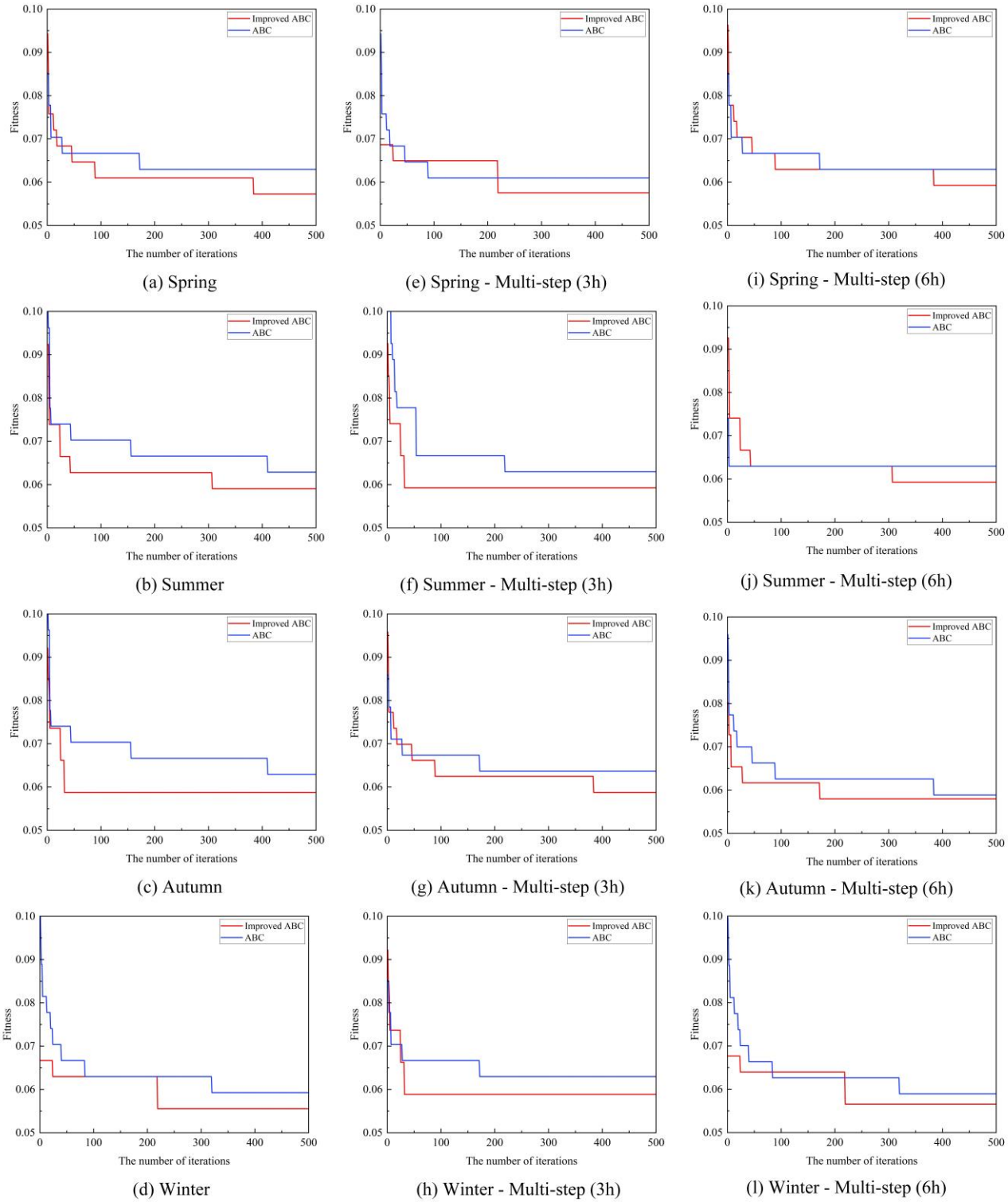

Figure 5. Comparison of performance.

Table 3. Optimal parameters of the loss function for different seasons in the inland region.

Season	Parameters of the loss function	Evaluation indices		
		MAE	MAPE	RMSE
Spring	$\alpha = 1.73, \beta = 0.53$	0.1011	0.1265	0.1163
Summer	$\alpha = 1.64, \beta = 0.60$	0.0990	0.0066	0.1136
Autumn	$\alpha = 1.5, \beta = 0.56$	0.0978	0.0088	0.1124
Winter	$\alpha = 1.81, \beta = 0.42$	0.0996	0.0824	0.1147

Table 4. Optimal parameters of the loss function for multi-step in the inland region.

Season	Step	Parameters of the loss function	Valuation index
			MSE
Spring	3 h	$\alpha = 1.53, \beta = 0.49$	0.0902
	6 h	$\alpha = 1.72, \beta = 0.65$	0.0881
Summer	3 h	$\alpha = 1.79, \beta = 0.58$	0.0838
	6 h	$\alpha = 1.91, \beta = 0.68$	0.0872

4.3. Analysis of comparative models in the inland wind farm

Due to the seasonal and regional characteristics of wind power generation, we verify the data in the four seasons of wind power inland. The threshold of the small fluctuation process is set at 0.2, and the threshold of the large fluctuation process is set at 0.8 in the inland region. Moreover, LSTM, a transformer, and temporal convolutional network (TCN) are analyzed as comparative models. Figure 6 shows the wind power forecast curves for different seasons inland. It can be seen that MI-PD-AdaBoost-LSTM has better prediction performance. Compared with LSTM, TCN, Transformer, and PD-AdaBoost-LSTM, the MAE of MI-PD-AdaBoost-LSTM decreased from 0.2444, 0.2369, 0.1984, 0.1778, and 0.1011 to 0.1011 in spring, as shown in Table 5. In winter, the MAE of MI-PD-AdaBoost-LSTM is 0.0996, 0.0990, and 0.0978 in winter, summer, and autumn, respectively. Furthermore, the comparison of the model prediction accuracy with different time delay is shown in Table 6. It can be seen that the meteorological data and power have an impact after a certain period of time, with the maximum reaching 64%. The performance of different models varies in different seasons. However, the MI-PD-AdaBoost-LSTM prediction algorithm has not decreased significantly. The robustness of the strategy proposed in this paper has been fully proved.

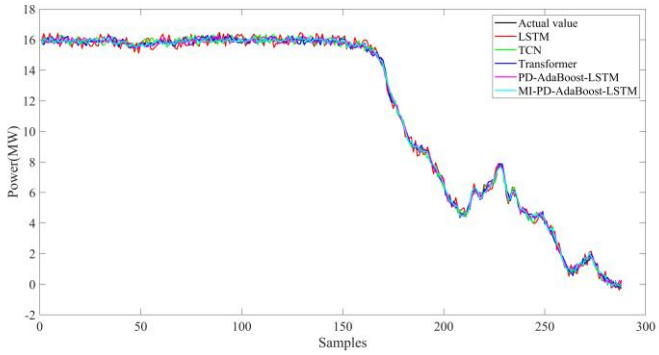

(a) Forecast results (Spring)

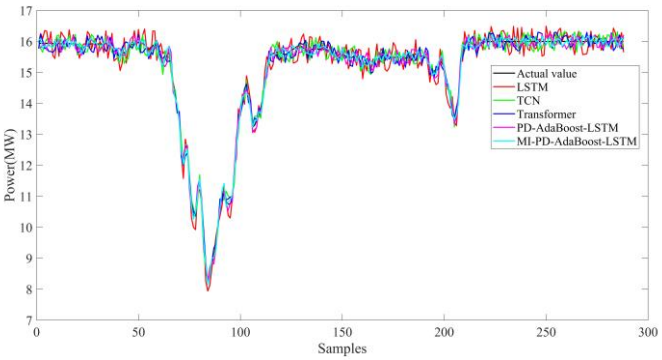

(b) Forecast results (Summer)

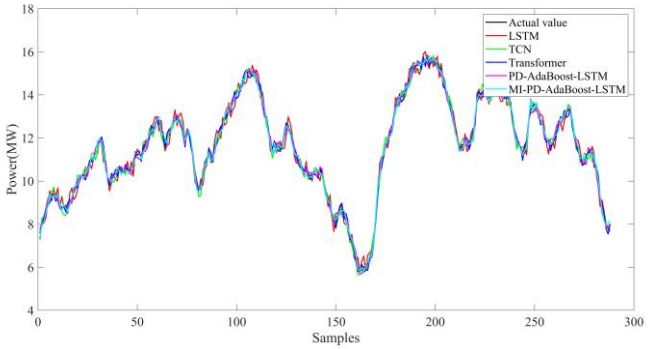

(c) Forecast results (Autumn)

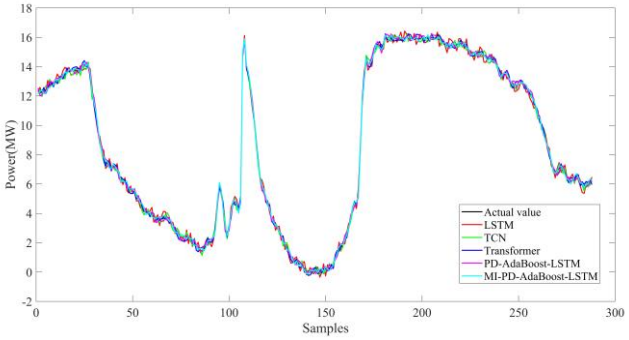

(d) Forecast results (Winter)

Figure 6. Comparison of different seasons in the inland region.

Table 5. Comparison of forecasts for different seasons in the inland region.

Season	Model	MAE	MAPE	RMSE
Spring	LSTM	0.2444	0.2947	0.2839
	TCN	0.2369	0.2820	0.2597
	Transformer	0.1984	0.2741	0.2301
	PD-AdaBoost-LSTM	0.1778	0.2956	0.2027
	MI-PD-AdaBoost-LSTM	0.1011	0.1265	0.1163
Summer	LSTM	0.2524	0.0169	0.2880
	TCN	0.2356	0.0157	0.2801
	Transformer	0.2408	0.0162	0.2712
	PD-AdaBoost-LSTM	0.1712	0.0115	0.1991
	MI-PD-AdaBoost-LSTM	0.0990	0.0066	0.1136
Autumn	LSTM	0.2514	0.0226	0.2882
	TCN	0.2321	0.0215	0.2520
	Transformer	0.2014	0.0192	0.2231
	PD-AdaBoost-LSTM	0.1830	0.0163	0.2084
	MI-PD-AdaBoost-LSTM	0.0978	0.0088	0.1124
Winter	LSTM	0.2422	0.1842	0.2792
	TCN	0.2223	0.1803	0.2675
	Transformer	0.1994	0.1757	0.2361
	PD-AdaBoost-LSTM	0.1822	0.1624	0.2088
	MI-PD-AdaBoost-LSTM	0.0996	0.0824	0.1147

Table 6. Comparison of forecasts for different time delays in the inland region.

Season	Model	time delay（−15 min）	time delay（+15 min）	optimal time delay
		MAE	MAE	MAE
Spring	MI-PD-AdaBoost-LSTM	0.1376	0.1320	0.1011
Summer	MI-PD-AdaBoost-LSTM	0.1003	0.1028	0.0990
Autumn	MI-PD-AdaBoost-LSTM	0.1274	0.1033	0.0978
Winter	MI-PD-AdaBoost-LSTM	0.1258	0.1137	0.0996

4.4. Analysis of multi-step prediction on an inland wind farm

The prediction accuracy over different times is analyzed in this section. The multi-time-scale predictions of LSTM, PD-AdaBoost-LSTM, TCN, Transformer, and MI-PD-AdaBoost-LSTM are compared. In this paper, wind power in spring and summer is predicted with time steps of 3 hours and 6 hours, respectively.

From Table 7 and Figure 7, all prediction performances decrease significantly as the prediction step size increases. In general, the prediction accuracy of MI-PD-AdaBoost-LSTM is higher than that of LSTM and PD-AdaBoost-LSTM. MI-PD-AdaBoost-LSTM fully extracts data features at short step sizes. With the increase in the step size, the prediction accuracy of MI-PD-AdaBoost-LSTM is also higher than that of the comparison model. Moreover, the LSTM and PD-AdaBoost-LSTM prediction performances under different seasons show little change.

Table 8 records the training time of the model with different prediction step sizes in the inland region, which is crucial for evaluating the efficiency and performance differences of the model. The proposed model is complex compared with other models. In spring, the training time of the proposed model is 34 minutes, which is 16 minutes longer than that of the Transformer model in a 3-hour step size. With a step size of 6 hours, the training time is 49 minutes. In summer, the training time of the model designed in this paper is 30 minutes in a 3-hour step size. With a step size of 6 hours, the training time is 42 minutes. The training time of the proposed model is longer than that of other comparison models. This is because the introduction of ABC leads to an increase in the training time. Moreover, the training time in spring is longer than that in summer due to the uncertainty of meteorological factors in spring. However, the proposed model can meet the requirements of the power grid under different prediction step sizes.

Table 7. Performance comparison of multi-step (3 and 6 h) in the inland region.

Season	Step	Model	RMSE
Spring	3 h	LSTM	0.1350
		TCN	0.1241
		Transformer	0.1204
		PD-AdaBoost-LSTM	0.1151
		MI-PD-AdaBoost-LSTM	0.0902
	6 h	LSTM	0.1451
		TCN	0.1362
		Transformer	0.1345
		PD-AdaBoost-LSTM	0.1343
		MI-PD-AdaBoost-LSTM	0.0881
Summer	3 h	LSTM	0.1250
		TCN	0.1123
		Transformer	0.1139
		PD-AdaBoost-LSTM	0.1083
		MI-PD-AdaBoost-LSTM	0.0838
	6 h	LSTM	0.1481
		TCN	0.1356
		Transformer	0.1294
		PD-AdaBoost-LSTM	0.1242
		MI-PD-AdaBoost-LSTM	0.0872

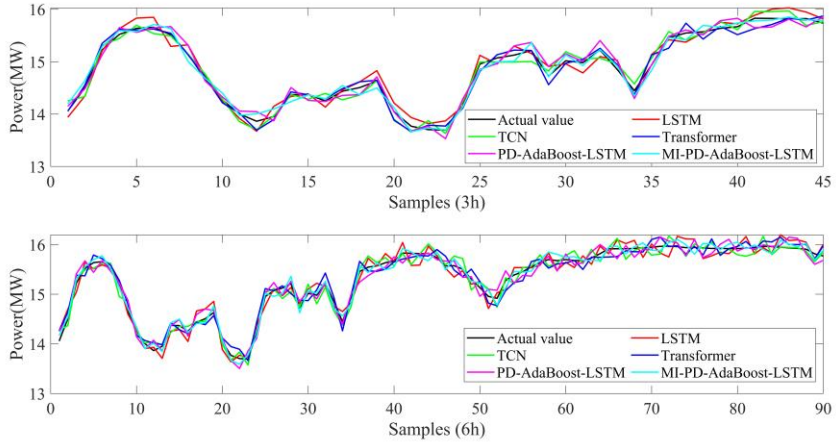

(a) Forecast Results of Multi-step Power in the Inland Region (Spring)

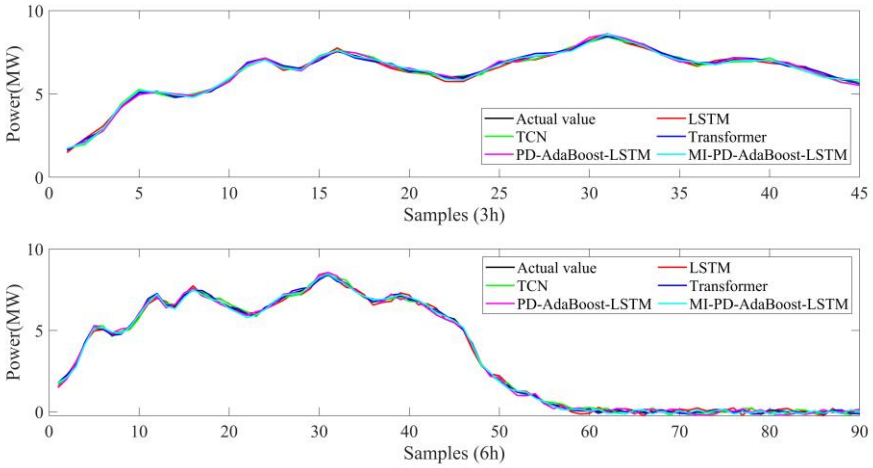

(b) Forecast Results of Multi-step Power in the Inland Region (Summer)

Figure 7. Multi-step power in the inland region.

Table 8. Analysis of model complexity and running time.

Season	Model	Running time (min)	
		3 h	6 h
Spring	LSTM	32	40
	TCN	26	31
	Transformer	18	25
	MI-PD-AdaBoost-LSTM	34	49
Summer	LSTM	28	39
	TCN	21	30
	Transformer	15	21
	MI-PD-AdaBoost-LSTM	35	42

4.5. Analysis of wind farms on coastal wind regions

The prediction results of the coastal areas are presented in Tables 9 and 10 and Figure 8, respectively. The meteorological data in coastal areas are different from those in inland areas. However, compared with other models, the model proposed in this paper also has advantages in coastal areas. However, compared with other models, the model proposed in this paper is superior in the coastal region.

Table 9. Comparison of forecasts for different seasons in the coastal region.

Season	Model	MAE	MAPE	RMSE
Spring	LSTM	0.2466	0.0792	0.2870
	TCN	0.1817	0.0537	0.2100
	Transformer	0.1443	0.0420	0.1675
	PD-AdaBoost-LSTM	0.1268	0.0356	0.1451
	MI-PD-AdaBoost-LSTM	0.0971	0.0292	0.1121
Summer	LSTM	0.2365	0.0152	0.2792
	TCN	0.1633	0.0105	0.1915
	Transformer	0.1556	0.0100	0.1769
	PD-AdaBoost-LSTM	0.1208	0.0078	0.1409
	MI-PD-AdaBoost-LSTM	0.1017	0.0066	0.1169
Autumn	LSTM	0.2480	0.1032	0.2870
	TCN	0.1735	0.0917	0.2015
	Transformer	0.1574	0.0740	0.1784
	PD-AdaBoost-LSTM	0.1248	0.0509	0.1444
	MI-PD-AdaBoost-LSTM	0.0950	0.0482	0.1111
Winter	LSTM	0.2532	0.1261	0.2792
	TCN	0.1908	0.1072	0.2675
	Transformer	0.1589	0.0652	0.2361
	PD-AdaBoost-LSTM	0.1278	0.0531	0.2088
	MI-PD-AdaBoost-LSTM	0.0981	0.0369	0.1147

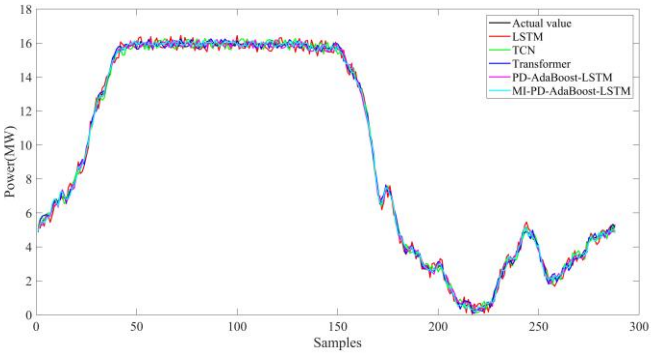

(a) Forecast results (Spring)

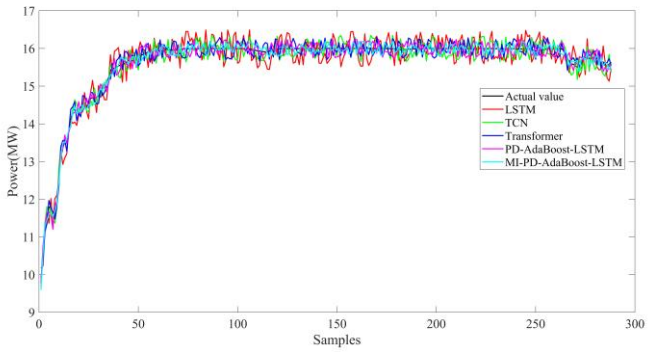

(b) Forecast results (Summer)

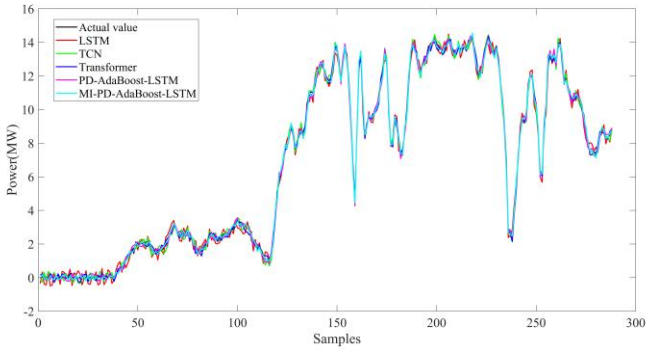

(c) Forecast results (Autumn)

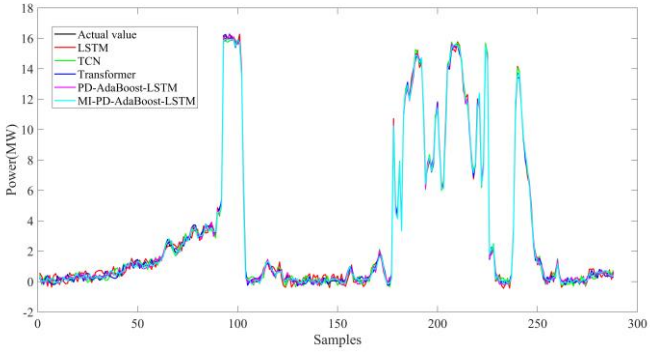

(d) Forecast results (Winter)

Figure 8. Comparison of different seasons in the coastal region.

Table 10. Performance comparison of multi-step (3 and 6 h) in the coastal region.

Season	Step	Model	RMSE
Spring	3 h	LSTM	0.1436
		TCN	0.1242
		Transformer	0.0860
		PD-AdaBoost-LSTM	0.0843
		MI-PD-AdaBoost-LSTM	0.0824
	6 h	LSTM	0.1474
		TCN	0.1162
		Transformer	0.1153
		PD-AdaBoost-LSTM	0.1096
		MI-PD-AdaBoost-LSTM	0.1084
Summer	3 h	LSTM	0.1349
		TCN	0.1282
		Transformer	0.1151
		PD-AdaBoost-LSTM	0.1044
		MI-PD-AdaBoost-LSTM	0.0837
	6 h	LSTM	0.1488
		TCN	0.1312
		Transformer	0.1235
		PD-AdaBoost-LSTM	0.1178
		MI-PD-AdaBoost-LSTM	0.0833

5. Conclusions

In this paper, the time delay and power characteristics of wind farm data are analyzed. The MI-PD-AdaBoost-LSTM is used to accurately predict wind power. In this paper, the time-delay calculation model is introduced into power prediction. The time feature between power and other variables is extracted. The recognition model of the power fluctuation process is established, and the division of the power fluctuation process is realized. The proposed model is tested on different regional seasons and multiple time scales. Compared with the traditional machine learning network, it is verified that the proposed model can be closer to the real application scenario. Moreover, the design model can meet the requirements of actual wind farm prediction. In future, the probabilistic or interval predictions method can be considered to ensure the actual operation requirements of the power system.

Use of AI tools declaration

I hereby declare that no AI tools were used in the completion of this work/project.

Acknowledgments

This work was supported by Basic Scientific Research Project of Liaoning Provincial Department of Education (JYTMS20230313).

Conflict of interest

The author declare that he has no known competing financial interests or personal relationships that could have appeared to influence the work reported in this paper.

References

1. Zhang Y, Kong X, Wang J, et al. (2024) Wind power forecasting system with data enhancement and algorithm improvement. *Renewable Sustainable Energy Rev* 196: 114349. https://doi.org/10.1016/j.rser.2024.114349
2. Tsai W, Hong C, Tu C, et al. (2023) A review of modern wind power generation forecasting technologies. *Sustainability* 15: 10757. https://doi.org/10.3390/su151410757
3. Hu Y, Liu H, Wu S, et al. (2024) Temporal collaborative attention for wind power forecasting. *Appl Energy* 357: 122502. https://doi.org/10.1016/j.apenergy.2023.122502
4. Tang Y, Yang K, Zhang S, et al. (2023) Wind power forecasting: A hybrid forecasting model and multi-task learning-based framework. *Energy* 278: 127864. https://doi.org/10.1016/j.energy.2023.127864
5. Huang Y, Liu GP, Hu W (2023) Priori-guided and data-driven hybrid model for wind power forecasting. *ISA Trans* 134: 380–395. https://doi.org/10.1016/j.isatra.2022.07.028
6. Nejati M, Amjady N, Zareipour H (2023) A new multi-resolution closed-loop wind power forecasting method. *IEEE Trans Sustainable Energy* 14: 2079–2091. https://doi.org/10.1109/TSTE.2023.3259939
7. Wang Y, Zhao K, Hao Y, et al. (2024) Short-term wind power prediction using a novel model based on butterfly optimization algorithm-variational mode decomposition-long short-term memory. *Appl Energy* 366: 123313. https://doi.org/10.1016/j.apenergy.2024.123313
8. Heinrich R, Scholz C, Vogt S, et al. (2024) Targeted adversarial attacks on wind power forecasts. *Mach Learn* 113: 863–889. https://doi.org/10.1007/s10994-023-06396-9
9. Gu G, Li N, Pan Y, et al. (2024) Wind power forecasting based on a machine learning model: considering a coastal wind farm in Zhejiang as an example. *Int J Green Energy* 21: 2551–2558. https://doi.org/10.1080/15435075.2024.2319228
10. Liao CW, Wang I, Lin KP (2021) A fuzzy seasonal long short-term memory network for wind power forecasting. *Mathematics* 9: 71–86. https://doi.org/10.3390/math9111178
11. Lin Q, Cai H, Liu H, et al. (2024) A novel ultra-short-term wind power prediction model jointly driven by multiple algorithm optimization and adaptive selection. *Energy* 288: 129724. https://doi.org/10.1016/j.energy.2023.129724
12. He Y, Zhu C, Cao C (2024) A wind power ramp prediction method based on value-at-risk. *Energy Convers Manage* 315: 118767. https://doi.org/10.1016/j.enconman.2024.118767

13. Wang C, Lin H, Hu H, et al. (2024) A hybrid model with combined feature selection based on optimized VMD and improved multi-objective coati optimization algorithm for short-term wind power prediction. *Energy* 293: 130684. https://doi.org/10.1016/j.energy.2024.130684
14. Sun B, Su M, He J (2024) Wind power prediction through acoustic data-driven online modeling and active wake control. *Energy Convers Manage* 319: 118920. https://doi.org/10.1016/j.enconman.2024.118920
15. Safari N, Chung CY, Price G (2018) A novel multi-step short-term wind power prediction framework based on chaotic time series analysis and singular spectrum analysis. *IEEE Trans Power Syst* 33: 590–601. https://doi.org/10.1109/TPWRS.2017.2694705
16. Zhou B, Ma X, Luo Y (2019) Wind power prediction based on LSTM networks and nonparametric kernel density estimation. *IEEE Access* 7: 165279–165292. https://doi.org/10.1109/ACCESS.2019.2952555
17. Wang J, Qian Y, Zhang L, et al. (2024) A novel wind power forecasting system integrating time series refining, nonlinear multi-objective optimized deep learning and linear error correction. *Energy Convers Manage* 299: 117818. https://doi.org/10.1016/j.enconman.2023.117818
18. Wang Y, Yang R, Sun L (2024) A novel structure adaptive discrete grey Bernoulli model and its application in renewable energy power generation prediction. *Expert Syst Appl* 255: 124481. https://doi.org/10.1016/j.eswa.2024.124481
19. Zhou H, Wang X, Zhu R (2022) Feature selection based on mutual information with correlation coefficient. *Appl Intell* 52: 5457–5474. https://doi.org/10.1007/s10489-021-02524-x
20. Belghit A, Lazri M, Ouallouche F, et al. (2023) Optimization of one versus All-SVM using AdaBoost algorithm for rainfall classification and estimation from multispectral MSG data. *Adv Space Res* 71: 946–963. https://doi.org/10.1016/j.asr.2022.08.075

AIMS Press